Molecular design enabled reduction of interface trap density affords highly efficient and stable perovskite solar cells with over 83% fill factor

Meng, Xiangyue; Ho, Carr Hoi Yi; Xiao, Shuang; Bai, Yang; Zhang, Teng; Hu, Chen; Lin, He; Yang, Yinglong; So, Shu Kong; Yang, Shihe

Authors

Xiangyue Meng, Carr Hoi Yi Ho, Shuang Xiao, Bai Yang, Teng Zhang, Chen Hu, He Lin, Yinglong Yang, Shu Kong So, and Shihe Yang

Author's Accepted Manuscript

Molecular Design Enabled Reduction of Interface Trap Density Affords Highly Efficient and Stable Perovskite Solar Cells with Over 83% Fill Factor

Xiangyue Meng, Carr Hoi Yi Ho, Shuang Xiao, Yang Bai, Teng Zhang, Chen Hu, He Lin, Yinglong Yang, Shu Kong So, Shihe Yang

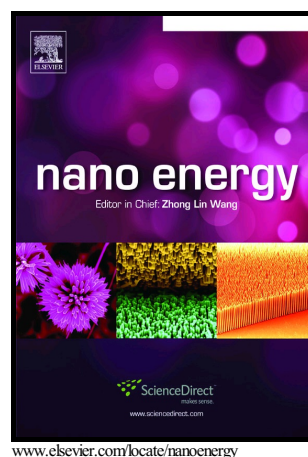Cite this article as: Xiangyue Meng, Carr Hoi Yi Ho, Shuang Xiao, Yang Bai, Teng Zhang, Chen Hu, He Lin, Yinglong Yang, Shu Kong So and Shihe Yang, Molecular Design Enabled Reduction of Interface Trap Density Affords Highly Efficient and Stable Perovskite Solar Cells with Over 83% Fill Factor, *Nano Energy,* https://doi.org/10.1016/j.nanoen.2018.07.063

This is a PDF file of an unedited manuscript that has been accepted for publication. As a service to our customers we are providing this early version of the manuscript. The manuscript will undergo copyediting, typesetting, and review of the resulting galley proof before it is published in its final citable form. Please note that during the production process errors may be discovered which could affect the content, and all legal disclaimers that apply to the journal pertain.

Molecular Design Enabled Reduction of Interface Trap Density Affords Highly Efficient and Stable Perovskite Solar Cells with Over 83% Fill Factor

Xiangyue Meng[a], Carr Hoi Yi Ho[b], Shuang Xiao[a], Yang Bai[a], Teng Zhang[a], Chen Hu[a], He Lin,[a] Yinglong Yang[a], Shu Kong So[b], Shihe Yang[a,c]*

[a]Department of Chemistry, The Hong Kong University of Science and Technology, Clear Water Bay, Kowloon, Hong Kong

[b]Department of Physics and Institute of Advanced Materials, Hong Kong Baptist University, Kowloon Tong, Hong Kong

[c]Guangdong Key Lab of Nano-Micro Material Research, School of Chemical Biology and Biotechnology, Shenzhen Graduate School, Peking University, Shenzhen 518055, China

chsyang@ust.hk (S. Y.).

Abstract

Advancing perovskite solar cell (PVSC) technologies toward its theoretical power conversion efficiency (PCE) and optimum stability requires stringent control over interfacial trap densities in

the devices. By introducing a new macromolecular interlayer material of PPDIN6 at the PCBM/Ag interface for planar p-i-n PVSCs, we succeeded in significantly reducing the trap density, thereby facilitating electron extraction and suppressing electron recombination at the interface. Consequently, a PCE of 20.43% was achieved with a record fill factor of 83.4%, which is one of the highest values for planar p-i-n PVSCs. Moreover, the amine groups in PPDIN6 could neutralize the migrating iodide ions and thus inhibit the formation of the insulating Ag-I bonds on the surface of the Ag electrode. As a result, we realized long-term stability for PPDIN6 based PVSCs, which maintained 85% of their initial performance after continuous operation at their maximum power point for 200 hours under 1-sun illumination in air with a relative humidity of 30%-50%.

Keywords

Perovskite solar cells; Trap density; Interlayer; Fill factor.

1. Introduction

Interface trap states, a form of localized electronic states, are regarded as one of the main limiting factors to high performance optoelectronic devices, such as solar cells, light emitting diodes, field effect transistors, photodetectors, etc. Suppressing or eliminating such trap states in optoelectronic devices through a simple and efficient approach is thus critical to the enhancement of device performance. Recently, the unique properties of organic-inorganic hybrid perovskite materials have made them a prime candidate for developing next generation photovoltaic cells [1-4]. Chiefly among the merits are broad and intense light absorption [5,6], appropriate direct band gaps [7,8], high charge carrier mobility and long charge carrier diffusion length even with a solution processed film [9-12]. In perovskite solar cells or any other solar

cells, charge extraction occurs at the interfaces, which may be particularly subject to recombination mainly due to any possible interfacial defects and the associated specific charge distributions [13]. On the way to highly efficient perovskite solar cells in the past few years, numerous works have mainly focused on the design of new materials and device structures [14,15], and the control over perovskite film quality [16-18]. It appears impending now that interface engineering has a big, untapped role to play for enhancing both efficiency and stability of perovskite solar cells [19,20].

Since the pioneering work by Miyasaka et al., the device structure of perovskite solar cell (PVSC) has evolved from a liquid electrolyte based perovskite sensitization scheme [21], to a solid hole-transporter based mesoporous structure [22], and to the present planar designs [23]. Of particular interest is the planar p-i-n architecture with a perovskite-fullerene planar heterojunction [24,25]. The planar p-i-n PVSCs have many advantages such as simple device fabrication, high stability and free of hysteresis [26-29]. However, interface barriers usually exist between the metal cathode (such as Ag, Al) and the electron transport layer (such as PCBM) in planar p-i-n PVSCs, leading to poor electron extraction [30,31]. Interface engineering should come to the rescue to eliminate any possible interfacial structural and electronic mismatches, to lower interfacial energy barriers, and thus to reduce interfacial trap density [32-35]. In addition to the aforementioned possible efficiency gain, interface engineering is also expected to improve the chemical stability of the perovskite absorber [36,37], thereby enhancing the overall device stability. Thus, it is essential to develop solution processed interlayer materials for highly efficient and stable planar p-i-n PVSCs, without using the more demanding thermal evaporation methods and complicated synthetic procedures [38].

3

In this work, we report the design of a tailor-made, amino-functionalized perylene diimide polymer (PPDIN6) and its demonstration as a new interlayer material for interface engineering in planar p-i-n PVSCs. With the device structure of $FTO/NiO/CH_3NH_3PbI_3/PCBM/PPDIN6/Ag$, we have achieved a PCE of up to 20.43% with a record fill factor of 83.4%, compared to only 17.38% PCE for the control device without PPDIN6. The remarkable performance enhancement is ascribed to the reduced trap density at the PCBM/Ag interface as elucidated by temperature dependent admittance spectroscopy measurement, which facilitated electron extraction and suppressed electron recombination at the PCBM/Ag interface. Moreover, the amine groups in PPDIN6 can neutralize the migrating iodide ions and inhibit the formation of the insulating Ag-I bonds on the surface of the Ag electrode, resulting in highly stable PVSC devices by inserting PPDIN6 between the PCBM layer and the Ag electrode.

2. Results and discussion

2.1 Design and Synthesis of PPDIN6

Figure 1a shows the molecular structure of the amino-functionalized perylene diimide polymer (PPDIN6), which has a backbone composition of alternate perylene-3,4,9,10-tetracarboxylic acid diimide (PDI) and a flexible amino-functionalized aliphatic segment. Several design considerations of PPDIN6 as the interlayer material are in order. First, PDI is a well-established n-type organic semiconductor with appropriate energy levels and high electron mobility needed for fluent electron transport [39,40]. Second, amine-functionalized aliphatic groups with an appropriate length are introduced to improve the solubility of PPDIN6 in the alcoholic solvent. Third, the amine group is selected because of its favorable interaction with Ag electrode as reported previously [41-43], which would help to reduce the interface trap density

4

and improve electron transport and extraction. Furthermore, the amine group is also expected to protect the metal electrode by extracting and stabilizing the iodide ions migrating from the perovskite layer [37]. Last but not least, PPDIN6 with the flexible polymer structure will enhance the film formation property, resulting in a well-covered and uniform film.

PPDIN6 was synthesized by one-pot reaction of perylene-3,4,9,10-tetracarboxylic dianhydride and pentaethylenehexamine in imidazole at 160 °C for 6 h. The raw product was washed by ethanol to remove excess imidazole. Advantageously, the polymerization process does not contain any metal catalyst, so no further procedure is needed to remove such deleterious catalyst residues. It should be noted that the synthesis and purification of PPDIN6 are very simple and easy to scale up, which are especially advantageous for commercial production.
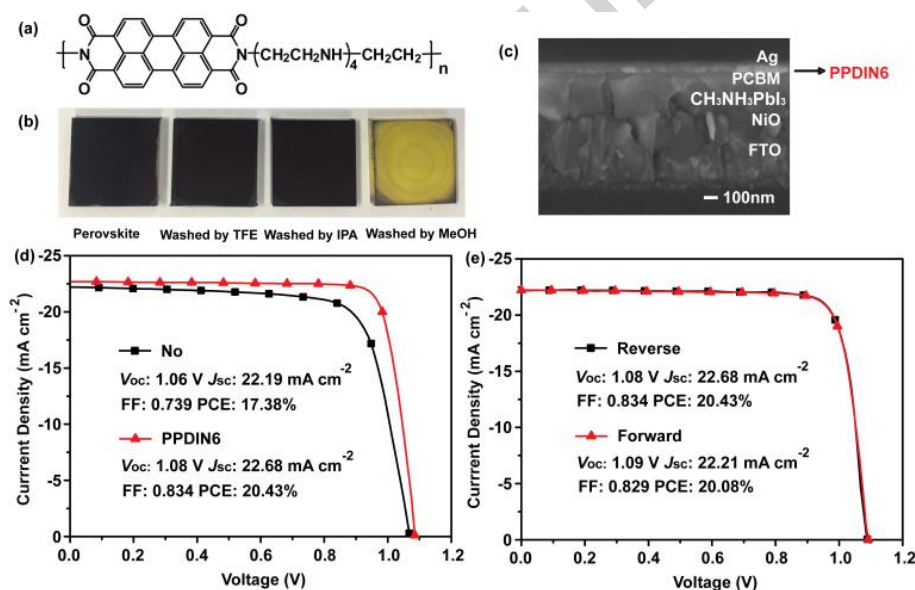
Figure 1 (a) The molecular structure of PPDIN6. (b) Photographs of pristine perovskite film and perovskite films after washed by different solvents. (c) The device configuration of the planar p-

5

i-n perovskite solar cell with PPDIN6. (d) *J-V* curves of the champion PVSCs prepared with or without PPDIN6. (e) *J-V* curves of the PVSCs based on PPDIN6 with the forward and reverse scan.

2.2 Solvent Selection

On a further note for processing the interlayer material of planar p-i-n perovskite solar cells, 2,2,2-trifluoroethanol (TFE) was introduced as a new solvent to dissolve PPDIN6 for perovskite solar cells. This choice is based on the fact that PPDIN6 is not soluble in isopropanol (IPA), and although methanol (MeOH) is a possible solvent for PPDIN6 (solubility < 0.5 mg/mL), it easily deteriorates the perovskite crystal structure and decomposes it to PbI_2. To study the effects of different solvents on the perovskite films, the films were washed by a series of alcoholic solvents, including TFE, IPA and MeOH (**Figure 1b**). The color of the perovskite films remained dark brown when washed by TFE or IPA, but the perovskite film turned into yellowish when washed by MeOH, indicating that the perovskite structure collapsed and was decomposed to PbI_2 (See Figure S2 and S3). TFE is the best solvent among the three commonly used solvents for processing the interlayer materials in PVSCs [41,43]. First, TFE with a large molecular size is difficult to break the perovskite crystal structure, making it a good orthogonal solvent for the perovskite film. Second, TFE is highly polar solvent due to the powerful electron-withdrawing property of trifluoro methyl group, which results in high solubility of PPDIN6 in TFE (higher than 5 mg/mL).

2.3 Photovoltaic Performance

In order to fully explore the potential of PPDIN6 as an interlayer material in perovskite solar cells, we incorporated the PPDIN6 interlayer material into the PCBM/Ag interface in a planar p-

i-n device configuration (**Figure 1c**). **Figure 1d** shows the current density-voltage (*J-V*) characteristics of the champion perovskite solar cells fabricated with or without PPDIN6. The control device without PPDIN6 exhibited a V_{oc} of 1.06 V, a J_{sc} of 22.19 mA cm^{-2}, a FF of 73.9% and a PCE of 17.38%. The unfavorable contact between the PCBM/Ag interface results in poor electron extraction. After inserting the PPDIN6 layer, the device showed a slightly higher V_{oc} of 1.08 V, a nearly J_{sc} of 22.68 mA cm^{-2}, a significantly increased FF of 83.4%, and a better PCE of 20.43%. The solar cell functionalized by PPDIN6 clearly shows improved fill factor, from 73.9% to 83.4%, which can be explained by reduced interface trap density as discussed later.

To investigate possible current hysteresis for our devices, the PPDIN6 based device was examined by varying the scan direction. As shown in **Figure 1e**, the reverse scan yielded a PCE of 20.43%, and the forward scan only showed a slightly lower PCE of 20.08%. This evidence clearly showed that no obvious current hysteresis was induced for the PPDIN6 based device. The steady state photocurrent output at the voltage close to the maximum power point (0.94 V) was measured. As shown in Figure S5, the current density for device based on PPDIN6 stays at about 21.6 mA cm^{-2} very steadily, corresponding to the PCE of 20.3%, which checks well with the small hysteresis and verifies the PCE value from the *J-V* curves. To check reproducibility of the device performance, PCE distributions were analyzed and collected for the PPDIN6 based PVSCs. As shown in Figure S6, the PCEs of PPDIN6 based devices range from 18% to 20.5%, with 70% of the measured devices showed PCE values of over 19%, indicating that PPDIN6 is a promising interlayer material for planar p-i-n PVSCs.

2.4 Trap Density Measurements
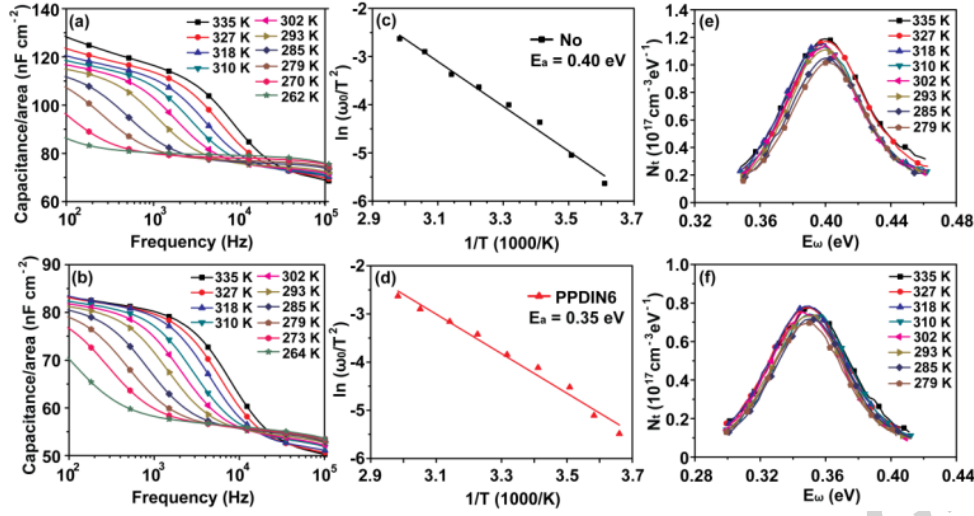
Figure 2 (a, b) Temperature dependent capacitance spectra, (c, d) Arrhenius plots of the characteristic transition frequencies and (e, f) the energetic defect distributions of the devices without (a, c, e) or with (b, d, f) PPDIN6.

Having established that PPDIN6 can improve the photovoltaic performance in planar p-i-n perovskite solar cells, we examine the effects of PPDIN6 modification on the trap density and the charge transport and recombination properties in the PVSC devices. The experiments include admittance spectroscopy (trap density measurement), dark J-V measurements of the electron only device and intensity modulated photovoltage spectroscopy (charge transport and recombination).

Temperature dependent admittance spectroscopy (AS) was performed accordingly to quantitatively estimate the trap density (N_t) in the PVSC devices (**Figure 2**). AS is a well-established, effective technique for characterizing both shallow and deep defects to analyze the N_t in perovskite solar cells [44-47]. **Figure 2a** displays the capacitance spectra measured at various temperatures (260 K to 335 K) in the dark from 10^2 to 10^5 Hz. An AC voltage of 50 mV

was used as an excitation signal and DC bias was kept at 0 V during the measurement. Firstly, the trap energy level (E_a) was derived via the relation:

$$\omega_0 = \beta T^2 \exp(\frac{-E_a}{K_b T})$$

where ω_0 is the characteristic transition (attempt to escape) frequency, β is temperature independent parameter, K_b is the Boltzmann constant, and T is the temperature, respectively. The trap density (N_t) can be derived pursuant to the equation:

$$N_t(E_\omega) = -\frac{V_{bi}}{e\,W}\frac{dC}{d\omega}\frac{\omega}{K_b T}$$

where V_{bi} is the built-in potential, C is the capacitance, ω is the applied frequency, e is the elementary charge, and W is the depletion width, respectively. The values of V_{bi} and W were obtained from the Mott - Schottky analysis. In the case of the PVSC device, the demarcation energy (E_ω) was determined by the applied angular frequency through the following expression:

$$E_\omega = K_b T \ln\frac{2\beta_c N}{\omega}$$

where β_c is the capture coefficient for the charge carriers, and N is the effective density of states in a given band in the PVSC device, respectively. Both β_c and N are temperature-independent, and their product was obtained by using E_a obtained above.

Figure 2a and **2b** demonstrate that as the frequency is decreased, deeper traps increasingly participate in the transitions, raising the capacitance. Moreover, the capacitance increases with temperature in the low frequency region (10^2 to 10^4 Hz); more precisely, the onset transition frequency increases with temperature. Instead of using the onset transition frequency, we define the characteristic transition frequency (ω_0) from the peak value of the [- $\omega \times dC/d\omega$] curve.

Indeed, ω_0 decreases with decreasing temperature as the onset transition frequency does. Clearly, as temperature is decreased, deep trap sites are frozen out, but rather shallow trap sites can still respond, resulting in gradually lower transition frequency. By plotting $\ln(\omega_0/T^2)$ *vs.* $1/T$, the slope gives the trap energy level (**Figure 2c** and **2d**). Interestingly, the device without PPDIN6 shows a trap energy level (E_a) at 0.40 eV, which is deeper than that with PPDIN6 (0.35 eV), meaning that some deep traps were eliminated by the introduction of PPDIN6. The energy distributions of the traps are shown in Figure 2e and 2f. For the device without PPDIN6 (**Figure 2e**), the energetic trap density distribution peaks at 1.2×10^{17} cm^{-3} eV^{-1}, while that of the device with PPDIN6 is reduced to 6.8×10^{16} cm^{-3} eV^{-1} (**Figure 2f**). The energetic spans of defect states can be fitted to a Gaussian distribution. The integrated trap density of the device without PPDIN6 is 7.6×10^{15} cm^{-3}, which is substantially higher than that with PPDIN6 (4.6×10^{15} cm^{-3}), signifying the role of PPDIN6 in trimming down the trap density.
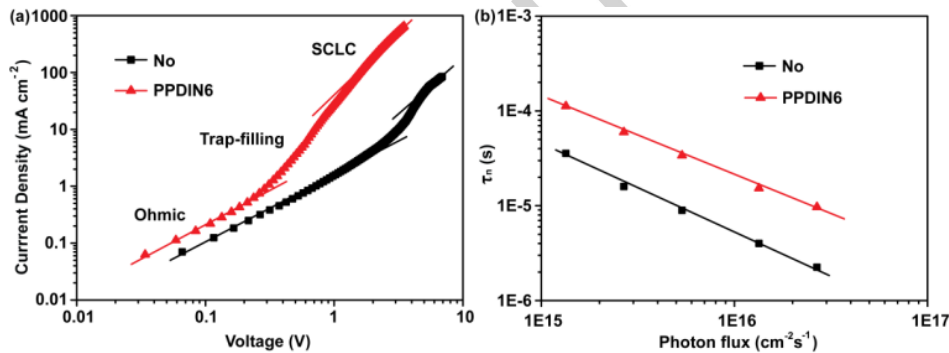
Figure 3 (a) Dark *J-V* curves of the electron-only devices with or without PPDIN6. (b) IMVS derived carrier lifetimes of the PVSC devices with or without PPDIN6.

To further study the effects of electron injection efficiency at the PCBM/Ag interface, we fabricated electron-only devices with the device configuration of ITO/ZnO/PCBM/(PPDIN6)/Ag, and the device dark current was measured to derive the electron

trap density. **Figure 3a** displays the dark J-V curves of the electron-only devices with or without PPDIN6 in a log-log scale. The dotted symbols are the experimental data points and the solid lines are a fit to $J \propto V^m$. At low voltages, the conduction is Ohmic with m = 1 for both devices with or without PPDIN6. In the medium voltage range, we can observe a steep rise in the current, indicating the presence of a trap-filling region. If charge traps are distributed in energy, they will be gradually filled with increasing electric field. Eventually the trap filled limit voltage (V_{TFL}) is reached, the current follows the trap-free Mott's V^2 law (SCLC region). The trap-filled limit voltage was determined by the trap density (N_t):

$$V_{TFL} = \frac{eN_t d^2}{2\varepsilon_r \varepsilon_0}$$

where e is the elementary charge, d is the thickness of PCBM, ε_r (= 3.9) is the relative dielectric constant of PCBM [48], ε_0 is the vacuum permittivity. Hence the electron trap density can be calculated from the trap-filled limit voltage. The V_{TFL} shifts to lower voltage with the modification of PPDIN6, implying lower electron trap density of the device with PPDIN6. The calculated electron trap density of the device with PPDIN6 was 5.0×10^{16} cm^{-3}, which is lower than that of the device without PPDIN6 (2.1×10^{17} cm^{-3}), thereby confirms the reduced trap density at the PCBM/Ag interface by introducing of PPDIN6. Moreover, the current density of the device with PPDIN6 is almost two orders of magnitude greater than that of the device without PPDIN6. This improvement in current density suggests that the modification with PPDIN6 reduces the injection barrier at the PCBM/Ag interface.

Intensity modulated photovoltage spectroscopy (IMVS) was also employed to evaluate the mean charge carrier life time of the PVSCs with or without PPDIN6 (**Figure 3b**), The electron lifetime (τ_n) can be obtained from the IMVS plot according to the equation: $\tau_n = 1/(2\pi f_{min(IMVS)})$,

where $f_{\min(IMVS)}$ represents the frequency at the minimum point on the IMVS complex plane plot. And the electron lifetime decreases as the incident light density increases because more light-induced photoelectrons at higher light density will increase the charge recombination rate. Most importantly, the electron lifetime of the PPDIN6 based device is almost five times higher than that without PPDIN6, regardless of the incident light density. A longer electron lifetime of the PPDIN6 based device indicates a lower recombination rate that occurs at the PCBM/Ag interface, which should be ascribed to the reduced trap density at the PCBM/Ag interface for the PPDIN6 based device.

2.5 Device Stability
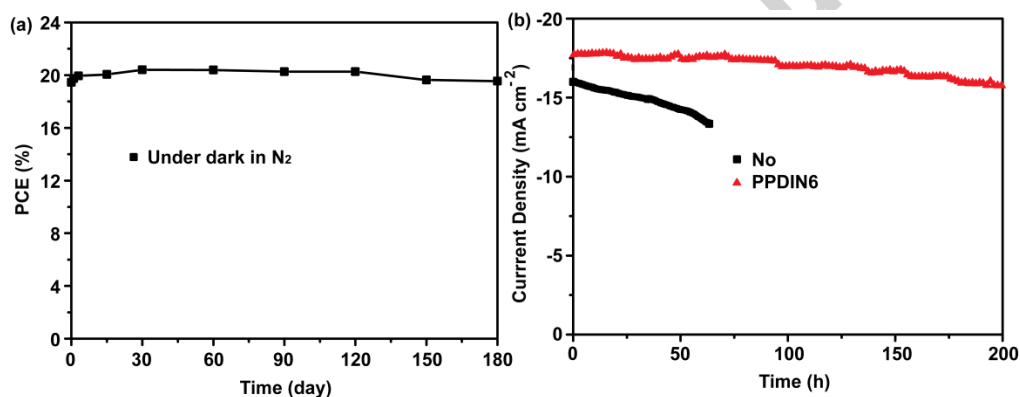
Figure 4 (a) Dark storage stability of encapsulated PPDIN6 based PVSCs in N_2 filled glovebox at room temperature. (b) Continuous maximum power point (MPP) tracking for 200 hours of the encapsulated cell with or without PPDIN6 under continuous one sun illumination (with a 420-nm cutoff UV filter) in air with a humidity of 30%-50%.

As another important benefit, the introduction of the PPDIN6 in PVSCs improves the device stability. As shown in **Figure 4a**, it was found that the PPDIN6 based device with proper encapsulation can maintain almost its original efficiency when stored in N_2 filled glovebox at

room temperature for 180 days. The long-term device operational stability of the PPDIN6-based PVSC under continuous one sun illumination (with a 420-nm cutoff UV filter) at the maximum power point (MPP) was also examined (**Figure 4b**). The PPDIN6 based solar cell with proper encapsulation retained 85% of its initial performance after continuous operation for 200 hours in air with a humidity of 30%-50%, as directly determined from the MPP tracking. While the device efficiency without PPDIN6 dropped quickly to 85% of its initial performance after continuous operation for 65 hours. It should be noted that previous long-term device operational stability test was always conducted in a nitrogen atmosphere, we conducted the test in air with a humidity of 30%-50% (See Table S1), which is closer to the actual solar cell operating conditions. Better stability would be achieved if the test is conducted in an inert atmosphere, or with Cs, Rb, FA and Br added to the perovskite layer [49-51]. As reported previously [37,52], the degradation of the PVSC devices might originate from the interfacial instability, which is likely caused by corrosive and mobile interstitial halide ions. The corrosive iodide ions in the perovskite layer easily migrate to the metal electrode (Ag or Al) through the PCBM layer and then contaminate the inner surface of the metal electrodes by forming an insulating metal halide compound (e.g., Ag-I). Importantly, the amine groups in PPDIN6 can neutralize the migrating iodide ions and inhibit the formation of the insulating Ag-I bonds on the surface of the Ag electrode, resulting in highly stable PVSC devices by inserting PPDIN6 into the PCBM/Ag interface.
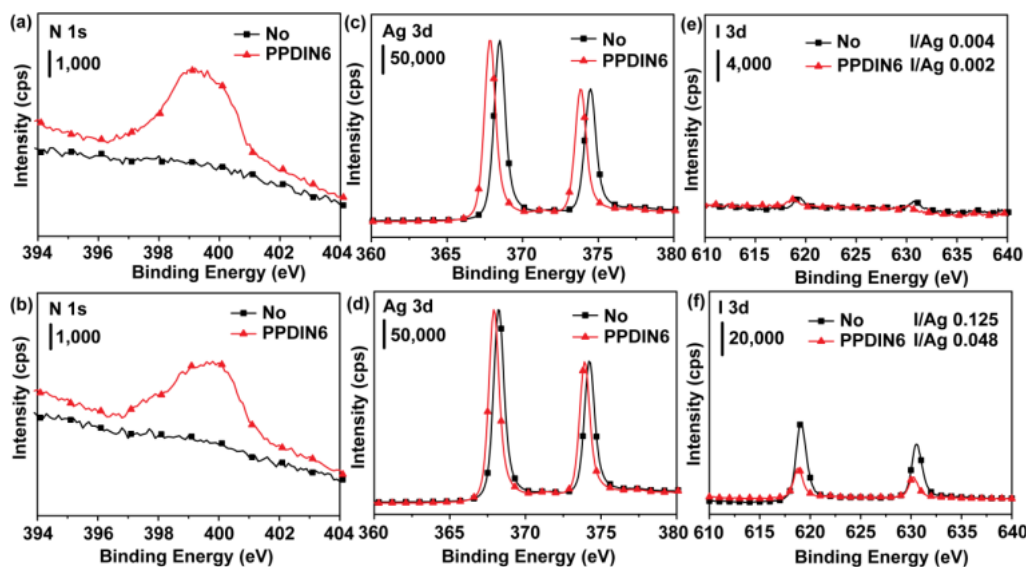
Figure 5 (a, b) N 1s (c, d) Ag 3d and (e, f) I 3d XPS spectra of (a, c, e) the fresh samples or (b, d, f) the samples after aging for ten days in N_2 filled glove box.

To obtain more direct evidence of the device stability, we further investigated the chemical properties of the device surface with the device structure of FTO/NiO/CH$_3$NH$_3$PbI$_3$/PCBM/ (PPDIN6)/Ag by X-ray photoelectron spectroscopy (XPS). The XPS samples were fabricated with a thin Ag (3 nm) layer atop to directly observe the interaction at the PCBM/Ag interface. To prove the electrode protection mentioned above, we carried out XPS measurements on the fresh samples and the samples after aging for ten days. For the fresh and aging samples with PPDIN6, a peak corresponding to N 1s was detected (**Figure 5a** and **5b**). The lone-pair electrons of nitrogen (N) from the amine groups in PPDIN6 were expected to interact with Ag to form the Ag-N bond. The binding energy of Ag 3d was observed to negatively shifted for the samples with PPDIN6 compared to those without PPDIN6 (Figure 5c and 5d), which confirms the existence of Ag-N bond. This Ag-N bond would facilitate electron extraction at the PCBM/Ag interface, and prevent Ag diffusion to form the insulating Ag-I bonds [37]. Moreover, the remaining pristine amine groups in PPDIN6 without interacted with Ag would neutralize the

migrating iodide ions and inhibit the formation of the insulating Ag-I bond at the Ag surface. For the fresh samples with or without PPDIN6, extremely low amount of I was observed, with I/Ag atomic ratio lower than 0.01 (Figure 5e). Considering that Ag was deposited by thermal evaporation, and the deposition thickness (3 nm) was well controlled with quartz crystal monitors, the amount of I can be represented by the atomic ratio of I/Ag obtained from XPS measurements. After aging for ten days in N_2 filled glove box, the sample without PPDIN6 showed a much higher atomic ratio of I/Ag (0.125, Figure 5f), resulting in the formation of a large amount of the insulating Ag-I bonds. Comparatively, for the sample with PPDIN6, a much lower atomic ratio of I/Ag (0.048) was detected because the corrosive iodide ions could be chemically neutralized by pairing with the amine groups in the PPDIN6 barrier layer and the metal contamination could be prohibited.

3. Conclusion

In summary, a solution-processed polymeric PPDIN6 was designed and successfully demonstrated as a very effective interlayer material for planar p-i-n PVSCs at the PCBM/Ag interface. With the device structure of FTO/NiO/CH$_3$NH$_3$PbI$_3$/PCBM/ PPDIN6/Ag, we were able to attain a PCE of up to 20.43% with a record fill factor of 83.4%. We have shown that PPDIN6 was able to effectively reduce the interface trap density, and to enhance the electron extraction at the PCBM/Ag interface. Moreover, we have successfully protected the metal electrode by adopting PPDIN6 as an efficient barrier layer to inhibit the migration of the iodide ions from the perovskite layer. Thus, we have realized planar p-i-n PVSCs with long-term operational stability that maintain nearly 85% of their initial PCEs after continuous operation at their maximum power point for 200 hours under 1-sun illumination in air with a humidity of 30%-50%. Together, our results provide an important guide for the molecular and material

15

designs toward stable and efficient PVSCs that may help to secure for the next-generation renewable energy source.

Acknowledgements

Appendix A. Supplementary material

Supplementary data associated with this article can be found in the online version at http://dx.doi.org/xxxxxxxx.

References

[1] M.A. Green, A. Ho-Baillie, H.J. Snaith, Nature Photon. 8 (2014) 506-514.

[2] S. Kazim, M.K. Nazeeruddin, M. Gratzel, S. Ahmad, Angew. Chem. Int. Ed. 53 (2014) 2812-2824.

[3] H.S. Jung, N.G. Park, Small 11 (2015) 10-25.

[4] Y.X. Zhao, K. Zhu, Chem. Soc. Rev. 45 (2016) 655-689.

[5] J.M. Ball, S.D. Stranks, M.T. Horantner, S. Huttner, W. Zhang, E.J.W. Crossland, I. Ramirez, M. Riede, M.B. Johnston, R.H. Friend, H.J. Snaith, Energy Environ. Sci. 8 (2015) 602-609.

[6] Q. Lin, A. Armin, R.C.R. Nagiri, P.L. Burn, P. Meredith, Nature Photon. 9 (2015) 106-112.

[7] J.H. Heo, D.H. Song, S.H. Im, Adv. Mater. 26 (2014) 8179-8183.

[8] N. Pellet, P. Gao, G. Gregori, T.-Y. Yang, M.K. Nazeeruddin, J. Maier, M. Grätzel, Angew. Chem. Int. Ed. 53 (2014) 3151-3157.

[9] G. Xing, N. Mathews, S. Sun, S.S. Lim, Y.M. Lam, M. Grätzel, S. Mhaisalkar, T.C. Sum, Science 342 (2013) 344-347.

[10] S.D. Stranks, G.E. Eperon, G. Grancini, C. Menelaou, M.J.P. Alcocer, T. Leijtens, L.M. Herz, A. Petrozza, H.J. Snaith, Science 342 (2013) 341-344.

[11] D. Shi, V. Adinolfi, R. Comin, M. Yuan, E. Alarousu, A. Buin, Y. Chen, S. Hoogland, A. Rothenberger, K. Katsiev, Y. Losovyj, X. Zhang, P.A. Dowben, O.F. Mohammed, E.H. Sargent, O.M. Bakr, Science 347 (2015) 519-522.

[12] Q. Dong, Y. Fang, Y. Shao, P. Mulligan, J. Qiu, L. Cao, J. Huang, Science 347 (2015) 967-970.

[13] J. Shi, X. Xu, D. Li, Q. Meng, Small 11 (2015) 2472-2486.

[14] M.M. Lee, J. Teuscher, T. Miyasaka, T.N. Murakami, H.J. Snaith, Science 338 (2012) 643-647.

[15] A. Mei, X. Li, L. Liu, Z. Ku, T. Liu, Y. Rong, M. Xu, M. Hu, J. Chen, Y. Yang, M. Grätzel, H. Han, Science 345 (2014) 295-298.

[16] J. Burschka, N. Pellet, S.-J. Moon, R. Humphry-Baker, P. Gao, M.K. Nazeeruddin, M. Gratzel, Nature 499 (2013) 316-319.

[17] N.J. Jeon, J.H. Noh, Y.C. Kim, W.S. Yang, S. Ryu, S.I. Seok, Nature Mater. 13 (2014) 897-903.

[18] W.S. Yang, J.H. Noh, N.J. Jeon, Y.C. Kim, S. Ryu, J. Seo, S.I. Seok, Science 348 (2015) 1234-1237.

[19] H. Zhou, Q. Chen, G. Li, S. Luo, T.-b. Song, H.-S. Duan, Z. Hong, J. You, Y. Liu, Y. Yang, Science 345 (2014) 542-546.

[20] Y. Bai, X. Meng, S. Yang, Adv. Energy Mater. 8 (2018) 1701883.

[21] A. Kojima, K. Teshima, Y. Shirai, T. Miyasaka, J. Am. Chem. Soc. 131 (2009) 6050-6051.

[22] H.-S. Kim, C.-R. Lee, J.-H. Im, K.-B. Lee, T. Moehl, A. Marchioro, S.-J. Moon, R. Humphry-Baker, J.-H. Yum, J.E. Moser, M. Grätzel, N.-G. Park, Sci. Rep. 2 (2012) 591.

[23] M. Liu, M.B. Johnston, H.J. Snaith, Nature 501 (2013) 395-398.

[24] J.-Y. Jeng, Y.-F. Chiang, M.-H. Lee, S.-R. Peng, T.-F. Guo, P. Chen, T.-C. Wen, Adv. Mater. 25 (2013) 3727-3732.

[25] Z. Zhu, Y. Bai, T. Zhang, Z. Liu, X. Long, Z. Wei, Z. Wang, L. Zhang, J. Wang, F. Yan, S. Yang, Angew. Chem. Int. Ed. 53 (2014) 12571-12575.

[26] L. Meng, J.B. You, T.F. Guo, Y. Yang, Acc. Chem. Res. 49 (2016) 155-165.

[27] X. Meng, Y. Bai, S. Xiao, T. Zhang, C. Hu, Y. Yang, X. Zheng, S. Yang, Nano Energy 30 (2016) 341-346.

[28] Y. Bai, S. Xiao, C. Hu, T. Zhang, X. Meng, Q. Li, Y. Yang, K.S. Wong, H. Chen, S. Yang, Nano Energy 34 (2017) 58-68.

[29] S. Xiao, Y. Bai, X. Meng, T. Zhang, H. Chen, X. Zheng, C. Hu, Y. Qu, S. Yang, Adv. Funct. Mater. 27 (2017) 1604944.

[30] C.C. Chueh, C.Z. Li, A.K.Y. Jen, Energy Environ. Sci. 8 (2015) 1160-1189.

[31] H. Kim, K.G. Lim, T.W. Lee, Energy Environ. Sci. 9 (2016) 12-30.

[32] J. Seo, S. Park, Y. Chan Kim, N.J. Jeon, J.H. Noh, S.C. Yoon, S.I. Seok, Energy Environ. Sci. 7 (2014) 2642-2646.

[33] Y. Hou, W. Chen, D. Baran, T. Stubhan, N.A. Luechinger, B. Hartmeier, M. Richter, J. Min, S. Chen, C.O.R. Quiroz, N. Li, H. Zhang, T. Heumueller, G.J. Matt, A. Osvet, K. Forberich, Z.-G. Zhang, Y. Li, B. Winter, P. Schweizer, E. Spiecker, C.J. Brabec, Adv. Mater. 28 (2016) 5112-5120.

[34] W. Chen, K. Sun, C. Ma, C. Leng, J. Fu, L. Hu, M. Li, M. Wang, Z. Zang, X. Tang, H. Shi, S. Lu, Org. Electron. 58 (2018) 283-289.

[35] L. Hu, K. Sun, M. Wang, W. Chen, B. Yang, J. Fu, Z. Xiong, X. Li, X. Tang, Z. Zang, S. Zhang, L. Sun, M. Li, ACS Appl. Mater. Interfaces 9 (2017) 43902-43909.

[36] W. Chen, Y. Wu, Y. Yue, J. Liu, W. Zhang, X. Yang, H. Chen, E. Bi, I. Ashraful, M. Grätzel, L. Han, Science 350 (2015) 944-948.

[37] H. Back, G. Kim, J. Kim, J. Kong, T.K. Kim, H. Kang, H. Kim, J. Lee, S. Lee, K. Lee, Energy Environ. Sci. 9 (2016) 1258-1263.

[38] Y. Liu, M. Bag, L.A. Renna, Z.A. Page, P. Kim, T. Emrick, D. Venkataraman, T.P. Russell, Adv. Energy Mater. 6 (2016) 1501606.

[39] J. Min, Z.-G. Zhang, Y. Hou, C.O. Ramirez Quiroz, T. Przybilla, C. Bronnbauer, F. Guo, K. Forberich, H. Azimi, T. Ameri, E. Spiecker, Y. Li, C.J. Brabec, Chem. Mater. 27 (2015) 227-234.

[40] Z. Hu, R. Xu, S. Dong, K. Lin, J. Liu, F. Huang, Y. Cao, Mater. Horiz. 4 (2017) 88-97.

[41] Q. Xue, Z. Hu, J. Liu, J. Lin, C. Sun, Z. Chen, C. Duan, J. Wang, C. Liao, W.M. Lau, F. Huang, H.-L. Yip, Y. Cao, J. Mater. Chem. A 2 (2014) 19598-19603.

[42] H. Zhang, H. Azimi, Y. Hou, T. Ameri, T. Przybilla, E. Spiecker, M. Kraft, U. Scherf, C.J. Brabec, Chem. Mater. 26 (2014) 5190-5193.

[43] H. Azimi, T. Ameri, H. Zhang, Y. Hou, C.O.R. Quiroz, J. Min, M. Hu, Z.-G. Zhang, T. Przybilla, G.J. Matt, E. Spiecker, Y. Li, C.J. Brabec, Adv. Energy Mater. 5 (2015) 1401692-n/a.

[44] M. Samiee, S. Konduri, B. Ganapathy, R. Kottokkaran, H.A. Abbas, A. Kitahara, P. Joshi, L. Zhang, M. Noack, V. Dalal, Appl. Phys. Lett. 105 (2014) 153502.

[45] Y. Shao, Z. Xiao, C. Bi, Y. Yuan, J. Huang, Nature Commun. 5 (2014) 5784.

[46] H.-S. Duan, H. Zhou, Q. Chen, P. Sun, S. Luo, T.-B. Song, B. Bob, Y. Yang, Phys. Chem. Chem. Phys. 17 (2015) 112-116.

[47] J.H. Heo, D.H. Song, H.J. Han, S.Y. Kim, J.H. Kim, D. Kim, H.W. Shin, T.K. Ahn, C. Wolf, T.-W. Lee, S.H. Im, Adv. Mater. 27 (2015) 3424-3430.

[48] F. Jahani, S. Torabi, R.C. Chiechi, L.J.A. Koster, J.C. Hummelen, Chem. Commun. 50 (2014) 10645-10647.

[49] M. Saliba, T. Matsui, J.-Y. Seo, K. Domanski, J.-P. Correa-Baena, M.K. Nazeeruddin, S.M. Zakeeruddin, W. Tress, A. Abate, A. Hagfeldt, M. Gratzel, Energy Environ. Sci. 9 (2016) 1989-1997.

[50] M. Saliba, T. Matsui, K. Domanski, J.-Y. Seo, A. Ummadisingu, S.M. Zakeeruddin, J.-P. Correa-Baena, W.R. Tress, A. Abate, A. Hagfeldt, M. Grätzel, Science 354 (2016) 206-209.

[51] H. Tan, A. Jain, O. Voznyy, X. Lan, F.P. García de Arquer, J.Z. Fan, R. Quintero-Bermudez, M. Yuan, B. Zhang, Y. Zhao, F. Fan, P. Li, L.N. Quan, Y. Zhao, Z.-H. Lu, Z. Yang, S. Hoogland, E.H. Sargent, Science 355 (2017) 722.

[52] J. Li, Q. Dong, N. Li, L. Wang, Adv. Energy Mater. (2017) 1602922.

Xiangyue Meng received his PhD degree from Institute of Chemistry Chinese Academy of Sciences in 2014. Now, he is visiting scholar in the Hong Kong University of Science and Technology (with Prof. Shihe Yang). Since 2014, he has been associate professor at Beijing University of Chemical Technology. His main research activities focus on the development of organic functional materials for various optoelectronic applications.

Carr Hoi Yi Ho is currently a Postdoctoral Research Scholar in Department of Materials Science and Engineering, North Carolina State University. He received his Ph.D. degree in Physics from Hong Kong Baptist University in 2017. His current research focuses on organic and perovskite electronic device physics and engineering.
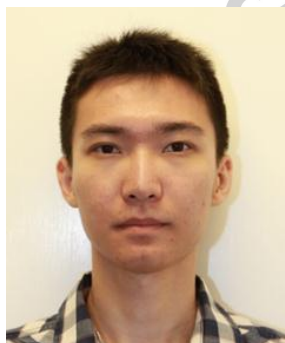
Yang Bai received his B.S. degree (2013) in School of Chemistry and Environment from Beihang University and his Ph.D. degree (2017) in Department of Chemistry from The Hong Kong University of Science and Technology. He is currently a postdoctoral fellow at The Hong
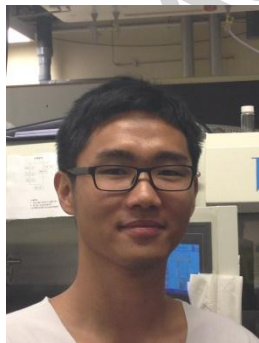
Kong University of Science and Technology. (Prof. Shihe Yang's group). His research focuses on perovskite solar cell, interface design and 2D material.

Shuang Xiao received his B.S. degree (2012) in School of Physics from Huazhong University of Science and Technology and Ph.D. degree (2017) in Department of Chemistry from The Hong Kong University of Science and Technology (HKUST) in China. He is currently a post-doctoral fellow in Professor Shihe Yang's group in Department of Chemistry from HKUST. His research focuses on perovskite solar cells, photoelectrochemical cells and catalysts.

Teng Zhang received his Ph.D. degree (2017) in School of Science from The Hong Kong University of Science and Technology. He is currently a post-doc researcher in Professor Shihe Yang's group from The Hong Kong University of Science and Technology. His current research focuses on solar conversion particularly perovskite solar cell and photoelectrochemical water splitting.

Chen Hu obtained his bachelor degree from a "2+2" program in Chemistry with The Hong Kong Polytechnic University associated with Sun Yat-Sen University. He is now working as a

research assistant in Professor Shihe Yang`s research group at Department of Chemistry in the Hong Kong University of Science and Technology with project on solution-processed perovskite solar cells.

He Lin received his B.S. degree (2015) in College of Chemistry and Life Science from Zhejiang Normal University. He is currently a Ph.D. candidate in Prof. Shihe Yang's group in Department of Chemistry of The Hong Kong University of Science and Technology. His current research focuses on hydrogen fuel generation by photoelectrochemical (PEC) water splitting.

Yinglong Yang acquired his B.S. degree in 2013 from University of Science and Technology of China. He is currently a Ph.D. candidate in Prof. Shihe Yang's group in Department of Chemistry of the Hong Kong University of Science and Technology. His current research focuses on carbon based perovskite solar cells.

Shu Kong So obtained his bachelor degree from Hamilton College and Ph.D. in Physics from Cornell University. He was a postdoctoral fellow in the Chemistry Department of the University of Toronto. In 1992, he joined the Department of Physics, Hong Kong Baptist University. Now he is the Associate Head of the Department, and the Program Director for the B.Sc. (Hons) Program in Physics and Green Energy. His major research interest is in the physics and the chemistry of thin film materials including transport and defect study of organic films, fabrication of organic solar cells and thin film transistors.

Shihe Yang is Professor at The Hong Kong University of Science and Technology. Now he is also Professor at the Shenzhen Graduate School, Peking University. He has contributed to cluster science, fullerenes and metallofullerenes, soft molecular interfaces and nanomaterials. His current research interests include the understanding, manipulation and applications of low-dimensional nanosystems and multiscale materials for energy conversion, particularly solar energy harvesting.

Highlights

- ·Design and synthesize a new macromolecular interlayer material of PPDIN6 at the PCBM/Ag interface for planar p-i-n PVSCs.
- ·Lower trap density in the PPDIN6 based PVSC device by performing temperature dependent admittance spectroscopy.
- ·High PCE with an over 83% fill factor was achieved with high device stability.

Graphical Abstract